ESTIMATION OF POSTMORTEM INTERVAL USING VARIOUS MARKERS IN THE LIVER OF ADULT ALBINO RATS (TARGETING PTEN/FASL SIGNALING PATHWAY)

Rabab Fawzy Hindawy[1], Eman Mohamed Faruk[2], Samia M Manawy[3], Basma A. Ibrahim[4], Doaa Elsayed Abdelrazzak[5], and Nahla Mohammed Ibrahim[5]

[1] Forensic Medicine and Clinical Toxicology Department, Faculty of Medicine Benha University, Egypt.

[2] Department of Anatomy, Faculty of Medicine, Umm Al-Qura University, Makkah, Saudi Arabia

[3] Anatomy and Embryology Department, Faculty of Medicine Benha University, Egypt.

[4] Medical Biochemistry and Molecular Biology Department, Faculty of Medicine, Zagazig University, Egypt.

[5] Forensic Medicine and Clinical Toxicology Department, Faculty of Medicine Zagazig University, Egypt.

Corresponding author: Nahla Mohammed Ibrahim, E-mail: drnahlaibrahimforensic@gmail.com, ORCID: 0009-0004-7238-0812.

Submit Date **2024-09-10**
Revise Date **2024-12-26**
Accept Date **2024-12-30**

ABSTRACT

Evaluation of period since mortality is one of the difficulties in forensic science. Autolysis triggers decomposition, which induces destructive cellular changes causing cell death. **Aim:** This work aimed to study mRNA expression depending on the process of cell death signaling, to evaluate alterations in antioxidant/oxidant variables and immunohistochemical postmortem changes in rats' livers. **Methodology:** Thirty-five rats have been classified into 5 groups. The liver was extracted at (0, 3, 6, 12, 24) hours postmortem, to measure the mRNA expression of FasL, PTEN, caspase-3, Bax, and Bcl2 by quantitative PCR in addition to MDA, CAT, GPx, and immunohistochemical postmortem changes. **Results:** MDA began to rise noticeably after death, CAT began to decline at 3 hours, and GPx declined at 6 hours. At three, six, twelve, and twenty-four hours, the FasL gene's relative expression in the liver of the rats was elevated. However, at twenty-four hours pm, it unexpectedly reduced. Also, the relative expression of the PTEN gene is elevated between three and twelve hours and reduced at twenty-four hours postmortem. Regarding mRNA concentrations of caspase-3 and Bax, a time-dependent increase was observed till twelve hours and a noticeable decline at twenty-four hours. Conversely, the Bcl2 gene's relative expression reduced between three- and twenty-four-hours postmortem. The early postmortem period was positively associated with the relative mRNA expression of FasL, PTEN, caspase-3, and Bax. The early postmortem period has been discovered to have a negative correlation with the relative expression of the Bcl2 gene. **Conclusion:** These findings supported our preliminary theory, since FasL, PTEN, caspase-3, Bax, and Bcl2 are involved in necrobiosis signaling mechanisms**.** They are possible candidates for assessing the period since death in 24-hour intervals or fewer. The oxidant/antioxidant and immunohistochemical changes in the liver of rats are also important to estimate the period after mortality. These biochemical indicators can be utilized to determine the early postmortem interval.

Keywords: adult albino rats, liver, postmortem interval, FasL, and PTEN.

INTRODUCTION:

The exact mortality period has been determined by a few straightforward observations, including livor mortis, algor mortis, and rigor mortis. Until recently, it has been impossible to accurately detect the exact period of mortality. The period of mortality has been determined by utilizing algorithms to determine the cooling behavior of the body, with the body temperature acting as the 1ry variable **(Youssef et al., 2019).**

An exact calculation of the period of mortality is crucial in the field of legal medicine because it's essential in the determination of appropriate civil repercussions and the elucidation of potential criminal behaviors. This is a critical responsibility in forensic studies **(Shaaban et al., 2017; Kaliszan and Wujtewicz, 2019),** and in each of the most challenging estimations to achieve **(Marhoff-Beard et al., 2018)**. Perpetrators' determination, witness declaration verification, and the reduction of the number of suspects may all be facilitated by a precise postmortem

interval (PMI). Additionally, investigators can reassemble conditions in the event of a homicide or suspicious death by possessing knowledge of PMI **(Zapico et al., 2014; Nolan et al., 2020)**.

Decomposition is a complex chemical and biological method that is influenced by a variety of environmental and personal factors. Consequently, numerous techniques utilized to identify a precise postmortem interval are characterized by substantial degrees of contradiction, uncertainty, and subjectivity **(Andersson et al., 2019; Connor et al., 2019)**.

In normal biological conditions, the balance among antioxidants and oxidants is in preference for antioxidants during life. Antioxidant systems regularly scavenge free radicals that are regularly produced in living tissue. The cellular components and metabolites will be damaged and liberated, resulting in a gradual destruction of the cells, as decomposition occurs approximately four minutes following mortality through autolysis. The body is unable to regulate the oxidant/antioxidant balance postmortem, resulting in biochemical aggravations **(Abo El Noor et al., 2016; Hegazy et al., 2020)**.

A better accurate indication of postmortem interval is provided by the disentanglement of molecular changes in the degradation of RNA, DNA, and protein. According to popular belief, RNA is more susceptible to disintegration compared to protein and DNA. This could assist in the accurate estimation of postmortem interval if RNA disintegration following mortality might be quantitatively identified **(Hegazy et al., 2020)**.

Fas Legend (FasL) and Phosphatase and tensin homolog (PTEN) are 2 genes that are involved in the controlling of a variety of processes cell, including apoptosis (known as programmed cell death), inflammation, growth, and migration of cells, invasion, and interactions with the extracellular matrix. This study demonstrated the regulatory role of FasL and PTEN in cell death by calculating their expression in association with the period following mortality **(Zapico et al., 2014)**.

The objective of the present investigation was to examine the early molecular, immunohistochemical, and biochemical postmortem modifications in rats' livers at zero, three, six, twelve-, and twenty-four-hours postmortem (hpm). Immunohistochemical investigations and quantitative PCR were conducted to investigate the mRNA expression of FasL, PTEN, caspase-3, Bax, and Bcl2, as well as the oxidant/antioxidant indicators.

MATERIAL AND METHODS

Animals

The research proposal has been accepted by the Research Ethics Committee at the Faculty of Medicine, Benha University (REC-FOMBU) in Benha, with permission number Rc.15.5.2024. The Animal Care Guidelines, estimated by the National Institutes of Health (NIH), were strictly followed during all techniques correlated to the handling and care of animals.

Adult albino rats (150–220 grams) have been obtained from the Experimental Animal Center of Benha, Faculty of Veterinary Medicine.

At the Anatomy and Embryology Department, Faculty of Medicine, Benha University, the animals underwent fourteen days of adaptation duration before the beginning of any experimental techniques. During the investigation, all rats were provided with standard laboratory chow and water adlibitum, and they were preserved at a standard room temperature of twenty-two to twenty-five degrees Celsius according to standard laboratory conditions.

According to **(Noshy, 2021),** 35 adult albino rats were randomly classified into 5 groups (7 animals each) which consisted of the control (group I) (G1) was sacrificed and the liver tissue was obtained promptly following mortality (zero-hour). G2, G3, G4, and G5 have been sacrificed, and the liver tissue has been obtained immediately following 3-, 6-, 12-, and 24- hpm, respectively. Albino rats were chosen because of their relatively similar enzymatic systems in liver tissue to humans.

The rats were euthanized by cervical dislocation after isoflurane 2% anesthesia. Subsequently, liver tissue samples were collected just after death, and liver specimens were taken from all rats at the specific period of the experiment, which was conducted at a temperature of twenty-five degrees Celsius. The samples have been classified into two parts. 1 part has been stored in a solution of neutral buffered formalin at a concentration of ten percent and utilized for histopathological examinations at the Histology and Cell Biology Department, Faculty of Medicine, Benha University. The other part was used for biochemical analysis at the Medical Biochemistry and Molecular Biology

Department, Faculty of Medicine, Zagazig University.

Biochemical Assays

Homogenate Tissue Analysis for Oxidative Stress Parameters

Following animal dissection, clots, and red blood cells were removed from the liver by perfusing them with a pH 7.4 phosphate-buffered saline (PBS) solution that included 0.16 milligrams per milliliter of heparin. Subsequently, the tissues were cryopreserved at minus eighty degrees Celsius for biochemical analysis. The procedure involved homogenizing one gram of tissue in five to ten milliliters of cold buffer (pH 7.5, fifty-millimeter potassium phosphate), centrifuging the mixture at 4000 rpm for 15 minutes while it was cooled, and then promptly analyzing the supernatant following the instructions provided with each kit. The concentration of malondialdehyde (MDA), a marker of oxidative stress, has been calculated following the manufacturer's instructions utilizing a bio-diagnostic kit (Cat. No. MD 2529, Egypt) for the thiobarbituric acid technique of **Ohkawa et al. (1979),** catalase (CAT) and glutathione peroxidase (GPx) antioxidant enzymes have been estimated utilizing commercial bio-diagnostic kits (Cat. No. CA 2517, Egypt) for CAT and (Cat. No. GP 2524, Egypt) for GPx, following the methodology of **Aebi (1984)** & **Paglia and Valentine (1967)**.

1.1.1. Gene Expression by quantitative Real-Time PCR

I. Total RNA Extraction from the Hepatic Tissue

The GENEzol^{TM} reagent (Cat. # GZR050, GZR100, GZR200) (Geneaid Biotch Ltd., Taiwan) and the manufacturer's instructions were utilized to extract total RNA from the liver tissue. The UV spectrophotometer's absorbance at 260/280 nanometer has been used to measure the integrity and purity of total RNA.

Reverse Transcription and cDNA Synthesis

The complementary DNA (cDNA) has been synthesized by reverse transcription of the isolated RNA utilizing TOPscriptTM RT DryMIX (dT18/dN6 plus) (enzynomics, Cat. # RT220-RT221) following the manufacturer's recommendations.

II. Real-Time Polymerase Chain Reaction for mRNA Gene Expression

The mRNA expression concentrations have been determined utilizing the Strata-geneMx3005P-qPCR System (Real-time PCR). The expression of the cellular housekeeping gene GAPDH has been utilized as a control. The primer sequences utilized in this examination are shown in **(Table 1).** 12.5 µL TOPreal™ qPCR 2X PreMIX (SYBR Green with low ROX) (Cat. # RT500S or RT500M) (Enzynomics, Korea), 1 µL of each primer (Invitrogen, USA), 5 µL cDNA, and 5.5 ddH2O have been utilized in the 25 µL PCR container. Following the 1st activation at ninety-five degrees Celsius for fifteen minutes, the amplification process consisted of forty cycles of denaturation at ninety-four degrees Celsius for fifteen seconds, annealing at sixty degrees Celsius for fifteen seconds, and elongation at seventy-two degrees Celsius for thirty seconds. The $2^{-\Delta\Delta CT}$ technique has been utilized to estimate relative gene expression as fold alteration **(Livak and Schmittgen, 2001)**.

Table 1. Sequences of primers.

Genes	Primer Sequences (5´ → 3´)	Accession number	Product length (bp)
FasL	Forward: CACCAACCACAGCCTTAGAGTATCA Reverse: ACTCCAGAGATCAAAGCAGTTCCA	NM_012908.1	171
PTEN	Forward: GGAAAGGACGGACTGGTGTA Reverse: TGCCACTGGTCTGTAATCCA	NM_031606.2	197
Caspase-3	Forward: GCAGCAGCCTCAAATTGTTGACTA Reverse: TGCTCCGGCTCAAACCATC	NM_012922.2	144
Bax	Forward: TGAAGACAGGGGCCTTTTTG Reverse: AATTCGCCGGAGACACTCG	NM_017059.2	140
Bcl2	Forward: ATGCCTTTGTGGAACTATATGGC Reverse: GGTATGCACCCAGAGTGATGC	NM_016993.2	120
GAPDH	Forward: AACTTTGGCATTGTGGAAGG Reverse: ACACATTGGGGGTAGGAACA	NM_017008.4	223

Histopathological Studies

The liver tissues have been dehydrated utilizing a series of alcohol solutions, starting with ninety percent alcohol, followed by absolute alcohol, and finally dipped in xylol. The liver has been embedded in paraffin wax to create blocks, which have been subsequently labeled and prepared. Sections with a thickness of five micrometers have been cut utilizing a rotatory microtome (LEICA RM 2125; UK). The sections have been affixed on slides and stained with Hematoxylin and Eosin. The stained sections have been photographed and examined.

Immunohistochemical Studies

The immunostaining methodology for CD86 and TGF in liver tissue involves meticulous steps, utilizing high-quality reagents for accurate results. Liver tissue sections were initially prepared and fixed, followed by deparaffinization and rehydration if applicable. Antigen retrieval is then carried out using the CD86 Antibody (Catalog #MA5-17031) from Thermo Fisher Scientific, ensuring optimal epitope exposure. To minimize non-specific binding, sections have been blocked with UltraVision Protein Block (Catalog #TA-125-PBQ) from Thermo Fisher Scientific. Subsequently, sections were incubated overnight at four degrees Celsius with 1ry antibodies targeting CD86 (Catalog #MA5-17031) and TGF (Catalog #MA5-18340) from Thermo Fisher Scientific. Following thorough washing, sections have been incubated with 2ry antibodies, such as Alexa Fluor® 488-conjugated Goat Anti-Rabbit immunoglobulin G (Catalog #A-11008) from Thermo Fisher Scientific, for fluorescent detection. Counterstaining, if desired, can be performed using a nuclear stain like DAPI. Finally, sections have been mounted with ProLong™ Gold Antifade Mountant (Catalog #P36930) from Thermo Fisher Scientific, enabling fluorescence preservation during imaging. Controls, including appropriate isotype controls, were included to validate staining specificity. The entire protocol was meticulously documented for reproducibility, ensuring accurate visualization and analysis of CD86 and TGF expression patterns in liver tissue samples **(Sanderson et al., 2019).**

The Morphometric Study

In the morphometric study of CD86 and TGF, digital image analysis is pivotal in quantifying their expression concentrations within liver tissue samples. Initially, tissue sections were immunostained for CD86 and TGF using specific antibodies, and high-resolution images were captured using a digital imaging system. These images were then processed utilizing Image-Pro Plus program version 6.0 (Media Cybernetics Inc., Bethesda, Maryland, USA), to quantify various morphometric parameters (quantified in 5 images from 5 non-overlapping fields of each rat). This includes measuring the area percentage occupied by CD86 and TGF staining within the tissue and assessing the intensity of staining as an indicator of protein expression concentrations.

Statistical Analysis

All the data obtained from the experiment has been noted and examined utilizing IBM SPSS Statistics software for Windows, Version 19 (IBM Corp., Armonk, NY, USA). The results from the experimental rats have been represented as mean ± standard deviation (SD) and subjected to one-way analysis of variance (ANOVA) and multiple comparisons post hoc test utilizing the statistical software program GraphPad Prism 8.0. Pearson's association coefficient (r) has been utilized to compare the relative expression of studied genes with the postmortem time. Results have been described as significant when $p<0.05$, statistically extremely significant when the p-value was less than 0.001, and insignificant at p-value was higher than 0.05.

RESULTS:

Biochemical Results

A comparison of the measured antioxidant and oxidant concentrations in the liver tissues between groups based on the time after death is shown in **(Table 2).** Every parameter demonstrated a statistically significant variance (p-value less than 0.05) among the groups. The oxidant biomarker (MDA) elevated statistically with time, while the antioxidants (CAT and GPx) reduced statistically with time. About 3 hours after death, MDA began to rise noticeably ($p<0.001$). Conversely, the antioxidants, CAT began to significantly decline at 3 hours after death ($p<0.001$), subsequently GPx at 6 hpm ($p<0.001$).

Table 2. Oxidative stress indicators in the rat's liver homogenate during the investigation period. (mean± standard deviation, number=seven)

	G1 **0h postmortem**	**G2** **3h postmortem**	**G3** **6h postmortem**	**G4** **12h postmortem**	**G5** **24h postmortem**
MDA (nmol/g.tissue)	0.96±0.06	1.05±0.18	1.84±0.07^{a**,b*}	4.12±0.47$^{(a,b,c)**}$	5.24±0.39$^{(a,b,c,d)**}$
CAT (U/g.tissue)	61.03±3.11	24.31±1.17^{a**}	14.40±0.50$^{(a,b)**}$	8.43±0.49$^{(a,b,c)**}$	5.01±0.43$^{(a,b,c)**,d*}$
GPx (U/g.tissue)	153.36±6.96	149.78±4.98	131.64±1.77$^{(a,b)**}$	43.89±2.88$^{(a,b,c)**}$	32.64±1.40$^{(a,b,c)**,d*}$

[a] Significant vs. G1, [b] significant vs. G2, [c] significant vs. G3, [d] significant vs. G4, [*] significant (p<0.05), [**] highly significant (p<0.001).

The relative expression of FasL gene in the rat's liver elevated postmortem, and a highly significant rise was observed in the relative expression of FasL at three, six, twelve-, and twenty-four- hpm, (p-value less than 0.001), than the G1 group (zero h postmortem). However, 24 h postmortem, mRNA concentrations suddenly decreased **(Fig. 1A).** The expression of the PTEN gene in the rat's liver initially elevated from three to twelve hours after death, then decreased at twenty-four hpm. Additionally, a significant rise was observed in the relative mRNA expression of PTEN at three, six, twelve- and twenty-four- hpm (p<0.001), compared with the G1 group **(Fig. 1B).** We discovered a similar pattern in mRNA concentrations of caspase-3 and Bax, a time-dependent raise was observed till twelve hpm and a noticeable decline at twenty-four hpm **(Fig. 1C&1D).** This quick decline in the mRNA concentrations is probably because of the destruction of RNA because of the advance of the autolysis pathway. Oppositely the relative expression of Bcl2 gene significantly reduced between three and twenty-four hpm, (p-value less than 0.001), compared with the G1 group **(Fig. 1E).**

A correlation was found between the early postmortem period and the results of mRNA concentrations. Nevertheless, associations were only carried out between 0- and 12 hours following death due to the abrupt decline after 24 hours **(Fig. 2, Table 3).** The relative mRNA expression of FasL, PTEN, caspase-3, and Bax demonstrated a powerful positive association with the early postmortem period (r = 0.9392, r = 0.9757, r = 0.9814, r = 0.9537, (p-value less than 0.001), respectively). Conversely, the relative expression of the Bcl2 gene has been observed to adversely associate intimately with the early postmortem time (r = - 0.8580, p<0.001). These findings supported our preliminary theory, since FasL, PTEN, caspase-3, Bax, and Bcl2 are involved in necrobiosis signaling mechanisms.

(A)

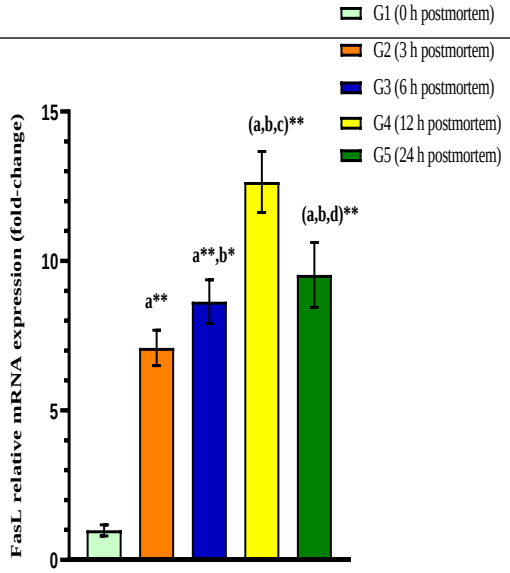
G1 (0 h postmortem)
G2 (3 h postmortem)
G3 (6 h postmortem)
G4 (12 h postmortem)
G5 (24 h postmortem)
FasL relative mRNA expression (fold-change)
15
10
5
0
a**
a**,b*
(a,b,c)**
(a,b,d)**

(B)

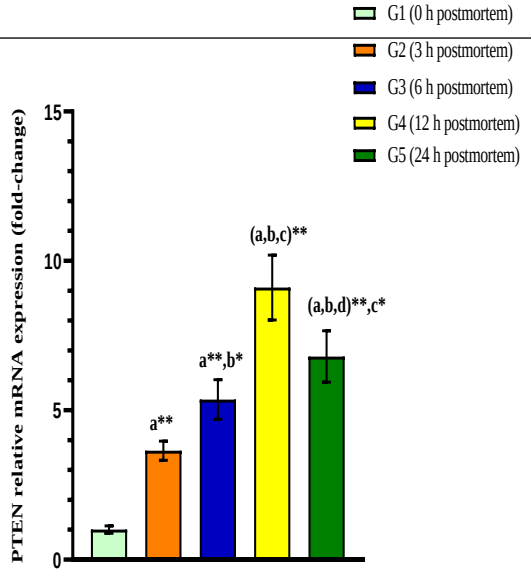
G1 (0 h postmortem)
G2 (3 h postmortem)
G3 (6 h postmortem)
G4 (12 h postmortem)
G5 (24 h postmortem)
PTEN relative mRNA expression (fold-change)
15
10
5
0
a**
a**,b*
(a,b,c)**
(a,b,d)**,c*

(C)

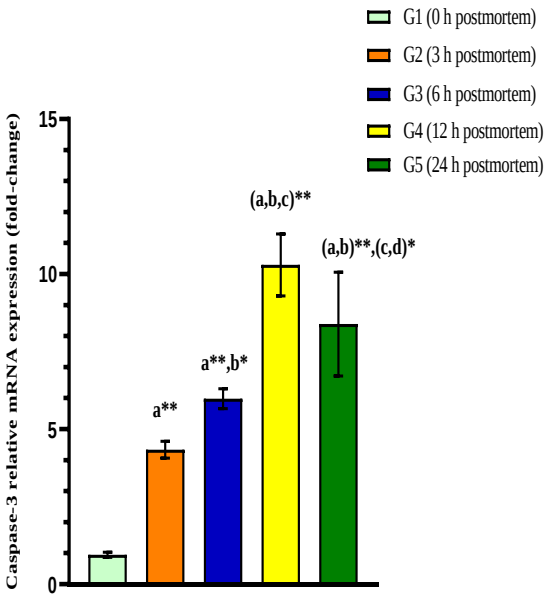
G1 (0 h postmortem)
G2 (3 h postmortem)
G3 (6 h postmortem)
G4 (12 h postmortem)
G5 (24 h postmortem)
Caspase-3 relative mRNA expression (fold-change)
15
10
5
0
a**
a**,b*
(a,b,c)**
(a,b)**,(c,d)*

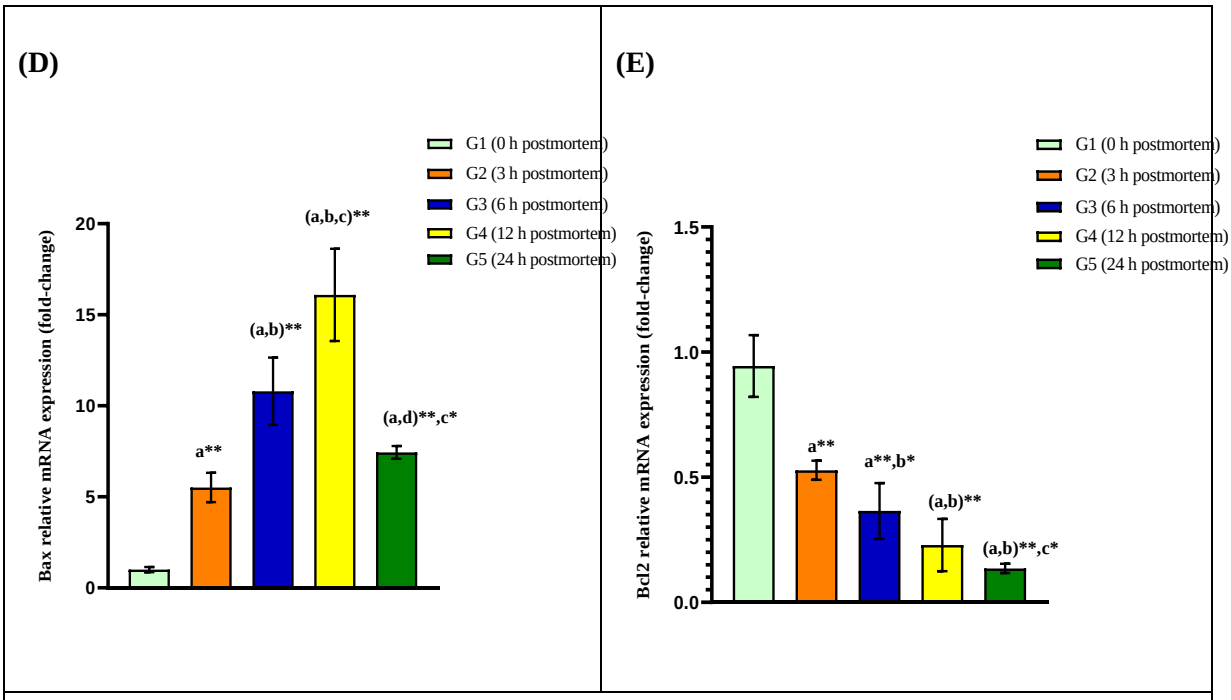

Fig. 1. Relative mRNA expression of FasL **(A)**, PTEN **(B),** Caspase-3 **(C),** Bax **(D),** and Bcl2 **(E)** in rats' liver tissues from 0 to 24 hours postmortem. [a] Significant vs. G1, [b] significant vs. G2, [c] significant vs. G3, [d] significant vs. G4, [*] significant (p<0.05), [**] highly significant (p<0.001).

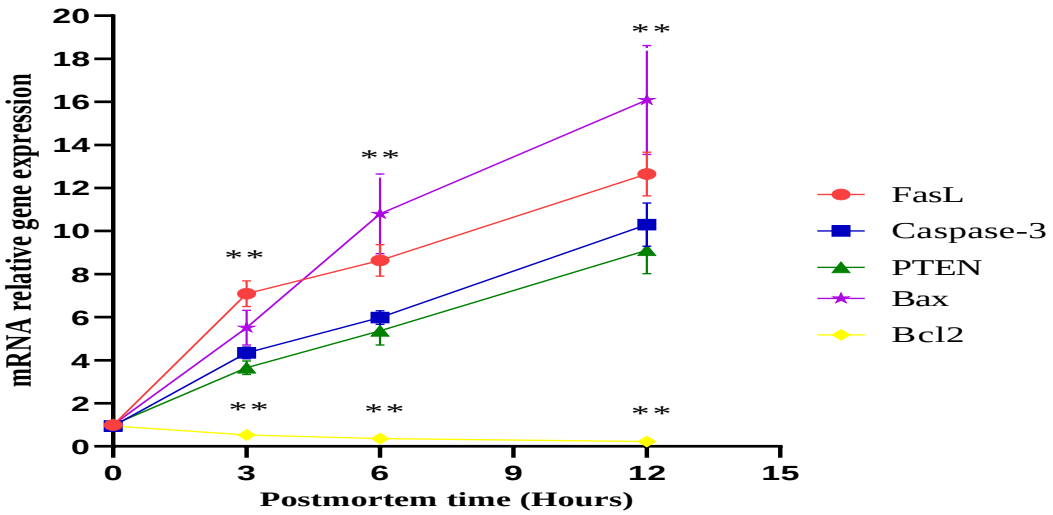

Fig. 2. Linear plot graph with error bars showing the relation between the early postmortem period and the mRNA relative expression of FasL, PTEN, Caspase-3, Bax, and Bcl2 genes in the rat's liver; data presented as mean ± SD (n=7 rats for each period point). Highly statistically significant variance from the G1 group (zero h postmortem) is defined as a p-value less than 0.001**.

Table 3. The association among the mRNA relative expression of the studied genes in rat's liver (y) and the postmortem time (x).

Genes	Equation	Pearson's correlation (r)	*P*-value
FasL	y= 0.8978x + 2.627	0.9392	<0.001**
PTEN	y= 0.6605x + 1.314	0.9757	<0.001**
Caspase-3	y= 0.7523x + 1.442	0.9814	<0.001**
Bax	y= 1.257x + 1.750	0.9537	<0.001**
Bcl2	y= -0.05496x + 0.8051	-0.8580	<0.001**

Histological Results

In group (1) In liver specimens, the hepatic lobules consist of cuboidal hepatocytes arranged in radiating cords, which are interspersed with blood sinusoids surrounding a central vein. The sinusoids, which are narrow blood spaces, are covered by phagocytic Kupffer cells and endothelial cells. The cytoplasm of the hepatocytes contained basophilic granules, and their nuclei were positioned in the center. The portal triad, which was located at the corners of the hepatic lobules, was composed of a bile ductule, a hepatic arteriole, and a large portal venule **(Fig. 3a)**.

In contrast, the other groups exhibited the following changes: The hexagonal structure of the hepatic lobules gradually disappeared, and the orderly arrangement of hepatocytes in cords was lost. The sinusoids morphology deteriorated progressively and eventually became unrecognizable. The sinusoids showed early signs of cell debris, mainly RBCs. Subsequently, the sinusoids' structure became indistinct, and debris from disintegrating hepatocytes has been evident. Detached hepatocytes were surrounded by this debris **(Fig. 3b&3c)**.

The hepatocyte nuclei underwent a distinct decomposition process, transitioning from clear to indistinct and becoming darker in color. The cytoplasm of the hepatocytes shows marked heterogeneity, with vacuoles and granules found in most specimens. The hepatocytes became detached from the hepatic cords at an early stage, scattering and being surrounded by cell debris. The peripheral portal areas, which are characterized by the presence of bile ducts and large blood vessels lined with columnar epithelium embedded in collagen, are frequently excellently maintained and decomposed more slowly than other structures in the liver (**Fig. 3d&3e).**

Immunohistochemical Results

TGF

The liver tissue at zero and three hours comprised hepatocytes and showed positive cytoplasmic and few nuclear TGF immunostaining **(Fig. 4a&4b)**. The liver tissue at 6 hours, 12 hours, and 24 hours showed weak to faint TGF immunostaining **(Fig. 4c&4d&4e).**

CD86

The liver tissue of G1 and G2 (at 0 and 3 hours) showed the hepatocyte with strong to moderate CD86 immunostaining **(Fig. 5a&5b)**. The liver tissue at 6 hours, 12 hours, and 24 hours showed weak to faint CD86 immunostaining **(Fig. 5c&5d&5e)**.

Morphometric Results

The Area parentage of TGF in the rat's liver decreased postmortem, and a highly significant reduction was observed in the relative expression of CD86 at three, six, twelve, and twenty-four hpm, (p<0.001), compared with the G1 group (zero-hour postmortem). However, 24 hours postmortem, CD86 concentrations suddenly decreased **(Fig. 6, Table 4)**.

A comparison of the measured area parentage concentrations in the liver tissues between groups based on the time after death. Area parentage of TGF and CD86 demonstrated a statistically significant variance (p-value less than 0.05) among the groups. The markers (TGF and CD86) were reduced statistically with time (p<0.001).

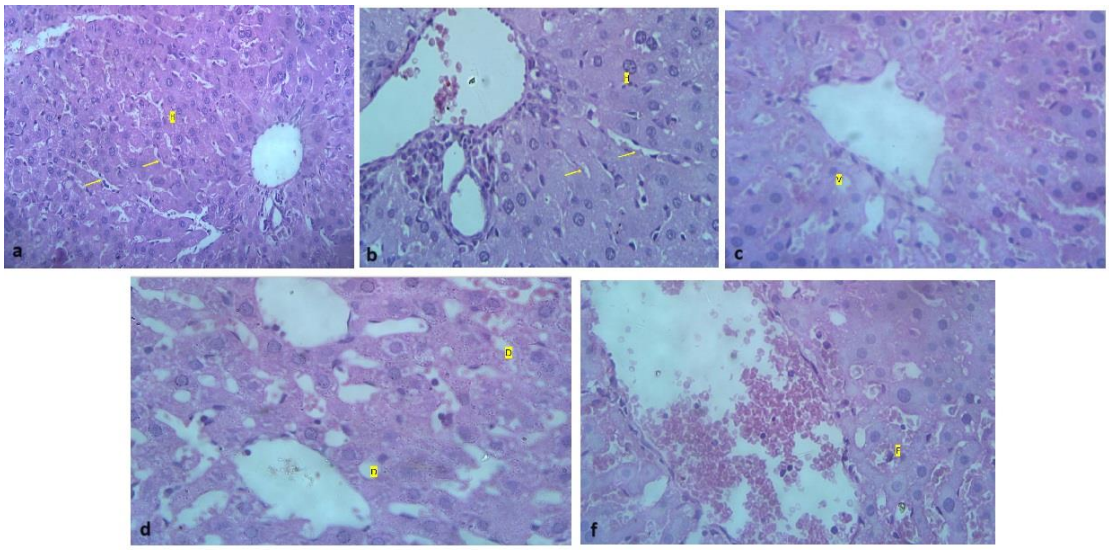

Fig. 3 (a&b). The liver tissue of G1and G2 (at zero and three hours) demonstrating; maintained cell structure and hepatic cords (H). The sinusoids are similarly distinct (arrow). **Fig. 3 (c)** The liver tissue at six hours showed vacuolar degeneration (V). **Fig. 3 (d)** The liver tissue at 12 hours showed hydropic degeneration (D) and early signs of decomposition with denser and darker cell nuclei. Note that detached hepatocytes. **Fig. 3 (e)** The liver tissue at twenty-four hours showed a deficiency of architecture (F) and decomposition of hepatocytes with cell debris, with extensive disintegration of the hepatocytes, and cell material deficiency. H&E Scale bar 100 um.

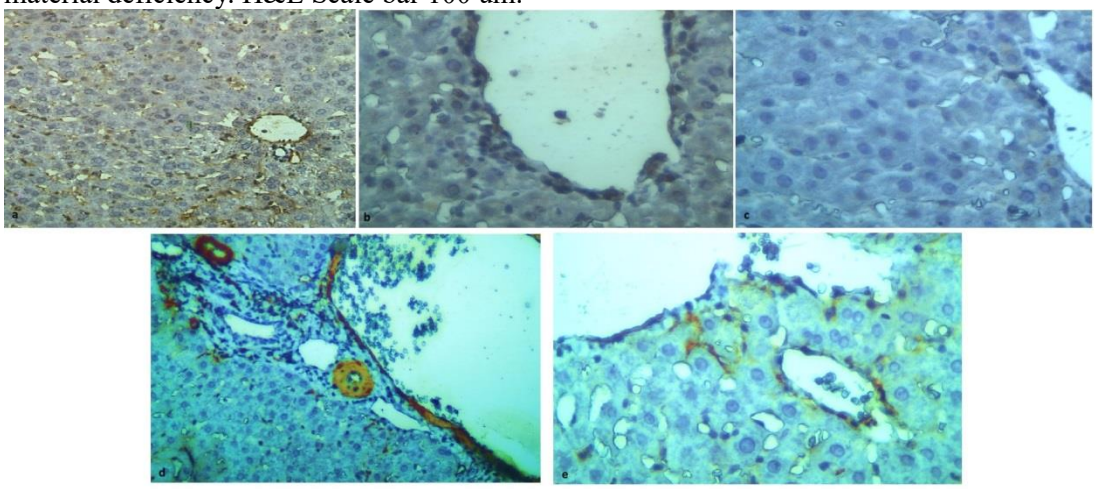

Fig. 4 (a&b). The liver tissue of G1 and G2 (at 0 and 3 hours) showing the hepatocyte with strong to moderate TGF immunostaining. **Fig. 4 (c&d&e)** The liver tissue at 6 hours, 12 hours, and 24 hours showed weak to faint TGF immunostaining. TGF immunostaining Scale bar 50um.

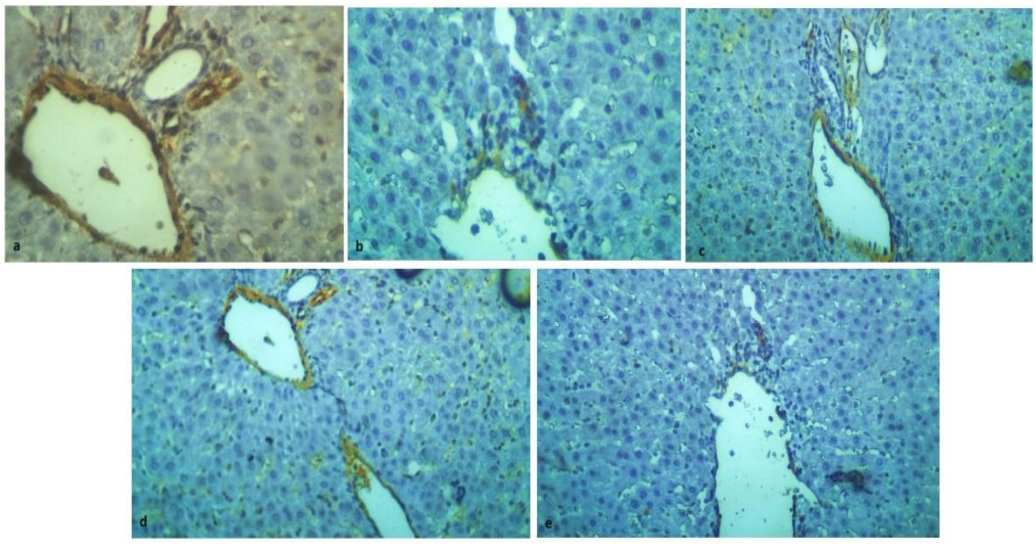

Fig. 5 (a&b). The liver tissue of G1 and G2 (at 0 and 3 hours) showed the hepatocyte with strong to moderate CD86 immunostaining. **Fig. 5 (c&d&e)** The liver tissue at 6 hours, 12 hours, and 24 hours showed weak to faint CD86F immunostaining. CD86 immunostaining Scale bar 50um.

Table 4. Area percentage of TGF and CD86 in rats' liver during the investigation period. (mean± standard deviation, number=seven)

	G1 **0h postmortem**	**G2** **3h postmortem**	**G3** **6h postmortem**	**G4** **12h postmortem**	**G5** **24h postmortem**
TGF	3.46±0.35	2.88±0.21	$1.81\pm0.50^{a^{**},b^{*}}$	$0.82\pm0.13^{(a,b,c)^{**}}$	$0.35\pm0.12^{(a,b,c,d)^{**}}$
CD86	22.25±1.28	$13.82\pm0.87^{a^{**}}$	$8.49\pm0.54^{(a,b)^{**}}$	$2.02\pm0.37^{(a,b,c)^{**}}$	$0.25\pm0.12^{(a,b,c)^{**},d^{*}}$

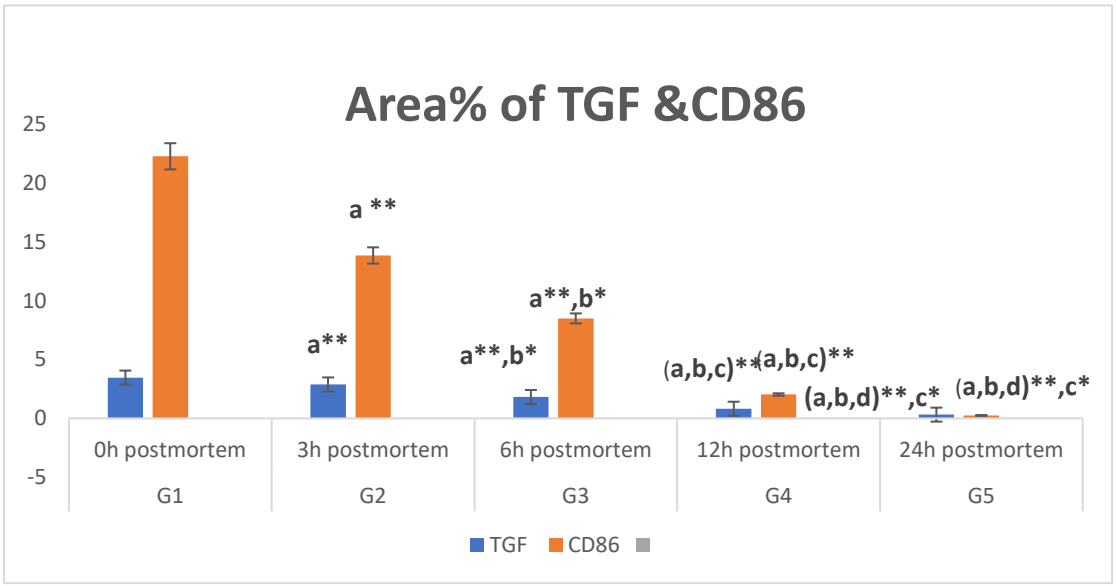

Fig. 6. Area percentage of TGF and CD86 in rats' liver tissues from 0 to 24 h postmortem.

DISCUSSION

The evaluation of parameters that are associated with the period following mortality is necessary for accurate determination of the postmortem interval. This definition is well-suited to the postmortem alteration of biochemical variables, as every alteration has its time factor **(Sampaio-Silva et al., 2013)**.

Iraz et al. (2006) & Aguilar et al. (2007) reported that the human body's oxidant/antioxidant defense system is distinguished by the development of free radicals and their subsequent elimination by the antioxidant system. A rise in oxidant concentrations and a reduction in antioxidant concentrations are found in injured tissues. It is impossible to suggest which body controls the oxidant/antioxidant equilibrium effectively following mortality, regardless of the viability of the cells in the early hours of death.

The results of the current research demonstrated that the measured time-dependent antioxidant and oxidant concentrations in the liver tissues following mortality revealed elevation of malondialdehyde about three hours after death. The elevated malondialdehyde concentrations with rising post-mortem interval help to elevated peroxidation of lipids that consequently results in elevated binding while detoxification by glutathione (GSH) which is finally decreased as observed by **Harish et al. (2011).**

In the research conducted by **Hegazy et al. (2020),** it was observed that the antioxidant concentrations of GSH, SOD, and CAT decreased significantly over time, with an increase in MDA that began on the first and continued until the six-hour postmortem. These outcomes are in line with the results of **Sener et al. (2012),** who discovered that both NO and malondialdehyde began to be significantly elevated at three to four hours in liver tissue after death.

In research conducted by **Abo El Noor et al. (2016)**, malondialdehyde began showing significant elevation in the heart tissue within the first three to four hours and in the kidney tissue within five to six hours after mortality. A significant increase was observed in NO at four to five hours in heart tissue and five to six hours following mortality in kidney tissue.

In the current work, the outcomes demonstrated a statistically significant decrease in the antioxidants; CAT and GPx with time as CAT began to significantly decline at 3 hours after death while GPx at 6 hpm. This is supported by the results reported by **Sakr et al. (2023)** who discovered a reduction in the concentration of glutathione reductase, glutathione peroxidase, and GSH with increasing PMI utilizing ELISA.

Research performed by **Li et al. (2006)** clarified that CAT concentration was significantly reduced at three to four hours following mortality in the brain. While in the liver, there was no significant decrease during the experiment period (8 hours). They attributed this to the presence of great levels of CAT in the kidney, liver, and erythrocytes while lesser levels are observed in the brain, heart, and skeletal muscle.

Sener et al. (2012) observed that the reduction in CAT concentration in rats' livers developed significantly at one to two hpm. **Abo El-Noor et al. (2016)** found that CAT concentration significantly reduced at six to seven and one to two hours following mortality in the kidney and heart, respectively. Their results were not in agreement with the results of **Harish et al. (2011)** who reported which tissue of the human brain showed insignificant change in activity of CAT with elevation postmortem interval.

In the current research, we used the analysis of the expression of genes, FasL, PTEN, caspase-3, Bax, and Bcl2 implicated in cell death for estimating the early PMI.

FasL is a member of the tumor necrosis factor family that stimulates cell death by attaching to its surface receptor Fas **(Nagata, 1999)**. PTEN has been known as a tumor inhibitor gene positioned on chromosome 10. It is deleted in numerous kinds of cell lines and human cancers. Moreover, PTEN contributes an essential part in apoptosis (programmed cell death) and regulation of cell growth **(Li and Sun, 1997; Tamura et al., 1999).**

Within our study, the relative expression of FasL gene in the rat's liver was elevated postmortem, and a highly significant rise was observed in the relative expression of FasL at three-, six-, twelve-, and twenty-four-hour postmortem, However, there was a sudden reduction twenty-four-hour postmortem.

The function of PTEN in the controlling of cell death was shown in the current research as the relative expression of PTEN gene in the liver of rats elevated between three to twelve hours after that a reduction at twenty-four-hour postmortem, and a significant

rise was observed in the relative mRNA expression of PTEN at three-, six-, twelve-, and twenty-four-hour postmortem. **Brunet et al. (1999)** clarified that by increasing its expression with the period following mortality, PTEN contributes to the controlling of death signals and FasL.

Caspase-3 is the most essential of the executioner caspases and is the primary cysteine protease that is shared in apoptosis. It is initiated by one of the caspases (caspase-10, caspase-9, or caspase-8). By cleaving the corresponding substrates in cells, it may stimulate the apoptosis pathway. Consequently, this protein is recognized as a "molecular switch." **(Sakahira et al., 1998; Fan et al., 2014)**.

The outcomes of the present work demonstrated a time-dependent raised pattern in mRNA concentrations of caspase-3 till twelve hpm and a noticeable decline at twenty-four hpm.

In line with the present work, **Saber and Ali (2016)** observed a time-dependent rise in mRNA concentrations of FasL, PTEN, and caspase-3 beginning 2 hours after death until 6 hours with a noticeable reduction at eighty hours following mortality. **Zapico et al. (2014)** attributed this quick decline in mRNA concentrations to the destruction of RNA as a result of the advance of the autolysis pathway.

Kavurma and Khachigian (2003) stated that the development of the mortality-inducing signaling complex (DISC) is initiated by the binding of Fas legend to the Fas receptor, which subsequently results in the activation of caspase-8. The effector caspase, caspase-3, is initiated by caspase-8 to stimulate the cell death signaling process. This event sequence clarifies the correlation among the expression concentrations of phosphatase and tensin homolog, FasL, and caspase-3 in our investigation, as the mRNA expression concentrations of these genes showed the same pattern.

In our work, the Bax increased till twelve hpm and the noticeable decline at twenty-four hpm. On the other hand, the relative expression of Bcl2 gene significantly decreased from three to twenty-four hpm.

Bax and Bcl2 are both members of the Bcl2 family, which is important in controlling the process of apoptosis. This family is composed of approximately fifteen genes; a few of them are pro-apoptotic, including Bax, whereas other genes are anti-apoptotic, including Bcl2. This discusses the reason for the variant in the expression concentrations of these genes in the present research **(Mund et al., 2003)**.

Research performed by **Noshy (2021)** similarly discovered that the expression concentration of the Bax gene showed an initial rise from three to eighteen hours, and then a subsequent reduction at twenty-four hours postmortem. Conversely, the Bcl2 gene demonstrated a gradual reduction in expression concentration from three to twenty-four hours following mortality in the liver of mice.

In the present study, a correlation was observed between the early postmortem period and the results of mRNA concentrations. Nevertheless, associations were only carried out between 0- and 12-hours following death due to the abrupt decline after 24 hours. The relative mRNA expression of FasL, PTEN, caspase-3, and Bax demonstrated a powerful positive association with the early postmortem time. Conversely, the relative expression of Bcl2 gene has been observed to adversely associate intimately with the early postmortem time. These findings supported the preliminary theory since these genes are involved in necrobiosis signaling mechanisms. In line with our findings, **Zapico et al. (2014) & Saber and Ali, (2016)** found a powerful positive linear association among mRNA concentrations of FasL, PTEN, and caspase-3 with time since death.

Undoubtedly, after death, all tissues succumb to autolysis, and estimating these alterations may be beneficial for identifying the mortality period, particularly when combined with additional techniques (**Karadžić et al., 2010)**.

In the current research, postmortem autolytic histological alterations were observed; the liver tissue of G1 and G2 (at 0 and 3 hours) showed maintained cell structure. In contrast, the other groups showed that the hexagonal structure of the hepatic lobules gradually disappeared, and hepatocytes were unable to maintain their regular arrangement in cords. The sinusoidal morphology deteriorated progressively and eventually became unrecognizable. Early indications of cell debris, particularly RBCs, have been found in the sinusoids. Later, the debris from disintegrating hepatocytes became readily apparent, with detached hepatocytes surrounded by this debris,

and the sinusoids' structure became indistinct, all these outcomes are in accordance with the results of **Ceciliason et al. (2021).**

According to the results discovered by **Karadžić et al.** (**2010)**, It was demonstrated that the period of post-mortem time influences the ultrastructural alterations of hepatocytes.

Our results revealed that by time the hepatocyte nuclei underwent a distinct decomposition process, transitioning from clear to indistinct and becoming darker in color. The cytoplasm of the hepatocytes showed marked heterogeneity, with vacuoles and granules found in most samples. Hepatocytes were found to be scattered and surrounded by cell debris as they detached from the hepatic cords at an early stage. Histopathological outcomes of the present research observed that the liver tissue at 6 hours showed vacuolar degeneration, while at 12 hours showed hydropic degeneration with H&E stain.

The liver's normal structure was apparent in sections obtained at the time of death. Pyknosis of certain nuclei was observed in the hepatocytes four hours postmortem. Swelling of the cytoplasm and pyknosis of the nuclei were elevated, respectively, at twelve- and twenty-four-hours postmortem. Hepatocyte lysis, complete lysis of red blood cells in the sinusoids, and the deficiency of cell outlines were noted between twenty-four - and seventy-two hours following mortality **(Yahia et al., 2018; Youssef et al., 2019)**.

The liver's structure deteriorated gradually, which correlated with the rise in oxidant concentrations and the reduction in antioxidant concentrations, as demonstrated by the present research, these results have been consistent with **Ozturk et al. (2013)** who stated that oxidant/antioxidant postmortem alterations have been correlated with the histopathological alterations in rat femoral muscle.

Lately, the focus of study on the calculation of the time since the mortality of a victim was on the identification of particular and reliable indicators **(Marrone et al., 2023)**.

The CD86 is one of the indicators correlated to immune activation of the cells (CD172α, CD163, CD206, CD200R, HLA-DR, CD86, and CD83) **(Sneeboer et al., 2019)**. The CD86 immunostaining liver tissue of G1 and G2 (at 0 and 3 hours) showed the hepatocyte with strong to moderate CD86 immunostaining, but at 6 hours, 12 hours, and 24 hours showing weak to faint CD86 immunostaining.

The tissue specimens have been preserved in formalin at varying PMI one day, two days, six days, and eight days) and immunohistochemical identifiers (CD117/c-kit, CD34, and CD56/N-CAM) have been utilized to collect specimens of skeletal striated muscle from four cadavers following autopsy **(Ceausu et al., 2016)**.

Lesnikova et al. (2018) concluded that Positive staining with KL1, S100, vimentin, and CD45 was observed in specimens from decedents with a PMI of one to three days while staining rates were reduced in specimens from decedents with a more prolonged PMI.

They discovered a tendency for an adverse association between postmortem interval and CD4+ due to the impact of the postmortem interval on the expression concentration of CD indicators in the colonic mucosa. Post-mortem tissue demonstrated lesser average values for the percentage of CD45-positive cells compared to the normal control. The ongoing changes in post-mortem tissue can indicate which postmortem interval has an inhibitory impact on the effector characteristics of cell-mediated immunity **(Zadka et al., 2021).**

The transforming growth factor (TGF) is used as a beneficial tool for the assessment of wound age in forensic practice. TGF-β1 is predominant in the healing process **(Soliman et al., 2024).** A critical objective of forensic pathology is to distinguish between vital skin wounds (antemortem lesions) and skin changes that happen following mortality. TGF and other agents are described to be beneficial for the differentiation of postmortem injuries from recent antemortem injuries **(Ros et al., 2022; Salerno et al., 2022; Tomassini et al., 2024).**

Tomassini et al. (2024) stated that after wound formation, mRNA expression of TGF-β1 and TNF-α elevated from 12 hours to the 7th day which has important value in wound repair.

The current study showed positive cytoplasmic and few nuclear TGF immunostaining of hepatic tissue at 0 and 3 hours. The liver tissue at 6 hours, 12 hours, and 24 hours showed weak to faint TGF immunostaining. Our morphometric results revealed a comparison of the measured area parentage concentrations in the liver tissues between groups based on the time after death. Area parentage of TGF and CD86 demonstrated a statistically significant variance among the groups. The markers (TGF and CD86) were reduced statistically with time.

The utilization of immunohistochemical techniques in putrefied corpses is difficult due to the change of the tissues, which may compromise the interpretation of the findings. However, they produced satisfactory leads to recently deceased bodies. The primary constraint associated with putrefaction is the degradation of protein molecules, which influences the antigens and determines their migration to a different location compared to the original. Furthermore, elevated binding of antibodies to the changed epitopes can result in a false positive in putrefied tissues. However, numerous investigations have managed the applicability of immunohistochemistry in various tissues of decomposed corpses and have determined which antigens may be detected despite the tissue's change. Immunohistochemistry's most significant applicability has been found in a PMI of three days **(Bertozzi et al., 2021).**

In general, the most reliable technique for precisely determining the time of mortality is the utilization of a multi-marker strategy. Nevertheless, additional study is required to determine an indicator that is both highly sensitive and specific for the assessment of the PMI.

CONCLUSION

The results of this research indicate that the antioxidants and oxidants in rats' liver change significantly in the 1st 24 hours following mortality. Also, the immunohistochemical alterations occurring in rat livers serve as a crucial tool for approximating the duration post-death. The current research similarly provided a quantitative tool for assessing the PMI till 24 hours following mortality through expression analysis of cell death genes. The mRNA expression concentrations of FasL, PTEN, caspase 3, Bax, and Bcl2 genes demonstrated a powerful association with the time since death between zero to twenty-four hours after death and these biochemical markers can be used to assess the early postmortem period.

Recommendations:

- The study parameters are recommended to be the subject of further studies on animals for longer periods (more than twenty-four hours), and on humans.
- Further studies are warranted to apply other cell death genes for extension of both period and precision of time since death estimation.
- Also, additional research should be conducted to consider various aspects related to the autolytic process that happens after death, including the manner and cause of mortality, air humidity, environmental conditions, and temperature.

Declaration of competing interest

The authors report no declaration of competing interest.

Funding information

The authors confirm that they weren't given any financial support for the conduct of this research.

Acknowledgment

The authors appreciate the assistance provided by the supporting team of colleagues and technicians.

REFERENCES

Abo El-Noor, M.M.; Elhosary, N.M.; Khedr, N.F. and El-Desouky, K.I. (2016). Estimation of Early Postmortem Interval Through Biochemical and Pathological Changes in Rat Heart and Kidney. The American Journal of Forensic Medicine & Pathology, 37(1), 40-46. https://doi.org/10.1097/PAF.0000000000000214

Aebi H. (1984): Catalase in vitro. Methods in enzymology, 105: 121–126. https://doi.org/10.1016/s0076-6879(84)05016-3

Aguilar, A.; Alvarez-Vijande, R.; Capdevila, S.; Alcoberro, J. and Alcaraz, A. (2007): Antioxidant patterns (superoxide dismutase; glutathione reductase; and glutathione peroxidase) in kidneys from non-heart-beating-donors: experimental study. Transplantation Proceedings, 39(1): 249–252. https://doi.org/10.1016/j.transproceed.2006.10.212

Andersson, M.; Ceciliason, A.; Sandler, H. and Mostad, P. (2019). Application of the Bayesian framework for forensic interpretation to casework involving postmortem interval estimates of decomposed human remains. Forensic Science International, 301, 402 - 414. https://doi.org/10.1016/j.forsciint.2019.05.050

Bertozzi, G.; Ferrara, M.; La Russa, R.; Pollice, G.; Gurgoglione, G.; Frisoni, P. and Cipolloni, L. (2021). Wound vitality in decomposed bodies: new frontiers

through immunohistochemistry. Frontiers in Medicine, 8, 802841. https://doi.org/10.3389/fmed.2021.802841

Brunet, A.; Bonni, A.; Zigmond, M.J.; Lin, M.Z.; Juo, P.; Hu, L.S.; Anderson, M.J.; Arden, K.C.; Blenis, J. and Greenberg, M.E. (1999). Akt promotes cell survival by phosphorylating and inhibiting a Forkhead transcription factor. Cell, 96(6), 857-68. https://doi.org/10.1016/S0092-8674(00)80595-4

Ceausu, M.; Hostiuc, S. and Dermengiu, D. (2016). Skeletal muscle satellite stem cells at different postmortem intervals. Romanian Journal of Legal Medicine, 24, 23-27. https://doi.org/10.4323/rjlm. 23

Ceciliason, A. S.; Andersson, M. G.; Nyberg, S. and Sandler, H. (2021). Histological quantification of decomposed human livers: a potential aid for estimation of the post-mortem interval? International Journal of Legal Medicine, 135(1), 253-267. https://link.springer.com/article/10.1007/s00414-020-02467-x

Connor, M.; Baigent, C. and Hansen, F. (2019). Measuring Desiccation Using Qualitative Changes: A Step Toward Determining Regional Decomposition Sequences. J. Foren. Sci., 64 (4), 1004-1011. https://doi.org/10.1111/1556-4029.14003

Fan, W.; Dai, Y.; Xu, H.; Zhu, X.; Cai, P.; Wang, L.; Sun, C.; Hu, C.; Zheng, P. and Zhao, B.Q. (2014). Caspase-3 modulates regenerative response after stroke. Stem Cells, 32(2), 473-86. https://doi.org/10.1002/stem.1503

Harish, G.; Venkateshappa, C.; Mahadevan, A.; Pruthi, N.; Bharath, M.M.S. and Shankar, S.K. (2011). Glutathione metabolism is modulated by postmortem interval, gender difference and agonal state in postmortem human brains. Neurochemistry International, 59(7), 1029–1042. https://doi.org/10.1016/j.neuint.2011.08.024

Hegazy, M.; Nasr, S. and Abdel Aziem, S. (2020). Ultrastructure of Cerebral Cortex Investigation during Early Postmortem Changes in a Rat Model. Indian Journal of Forensic Medicine and Pathology, 13(3), 365-376. http://dx.doi.org/10.21088/ijfmp.0974.3383.13320.1

Iraz, M.; Ozerol, E.; Gulec, M.; Tasdemir, S.; Idiz, N.; Fadillioglu, E.; Naziroglu, M. and Akyol, O. (2006). Protective effect of caffeic acid phenethyl ester (CAPE) administration on cisplatin-induced oxidative damage to liver in rat. Cell Biochem Funct, 24(4), 357–361. https://doi.org/10.1002/cbf.1232

Kaliszan, M. and Wujtewicz, M. (2019). Eye temperature measured after death in human bodies as an alternative method of time of death estimation in the early postmortem period. A successive study on new series of cases with exactly known time of death. Legal Medicine, 38, 10–13. https://doi.org/10.1016/j.legalmed.2019.03.004

Karadzic, R.; Ilic, G.; Antovic, A. and Banovic, L. K. (2010). Autolytic ultrastructural changes in rats and human hepatocytes. Romanian Journal of Legal Medicine, 18(4), 247-252. https://cir.nii.ac.jp/crid/1363388845943240576

Kavurma, M.M. and Khachigian, L.M. (2003). Signaling and transcriptional control of Fas ligand gene expression. Cell Death Differ.; 10(1), 36-44. https://www.nature.com/articles/4401179

Lesnikova, I.; Schreckenbach, M. N.; Kristensen, M. P.; Papanikolaou, L. L. and Hamilton-Dutoit, S. (2018). Usability of immunohistochemistry in forensic samples with varying decomposition. The American Journal of Forensic Medicine and Pathology, 39(3), 185-191. https://doi.org/10.1097/PAF.0000000000000408

Li, D. M and Sun, H. (1997). TEP1, encoded by a Candidate Tumor Suppressor Locus, is a Novel Protein Tyrosine Phosphatase Regulated by Transforming Growth Factor β. Cancer Research, 57(11), 2124-9. https://aacrjournals.org/cancerres/article/57/11/2124/503196/TEP1-Encoded-by-a-Candidate-Tumor-Suppressor-Locus

Li, G.; Sang, N. and Guo, D. (2006). Oxidative damage induced in hearts, kidneys and spleens of mice by landfill leachate. Chemosphere, 65(6), 1058–1063. https://doi.org/10.1016/j.chemosphere.2006.02.056

Livak, K. J. and Schmittgen, T. D. (2001).

Analysis of relative gene expression data using real-time quantitative PCR and the 2 (-Delta Delta C(T)) Method. Methods (San Diego, Calif.), 25(4), 402–408. https://doi.org/10.1006/meth.2001.1262

Marhoff-Beard, S.; Forbes, S. and Green, H. (2018). The validation of 'universal' PMI methods for the estimation of time since death in temperate Australian climates. Forensic Science International, 291, 158–166. https://doi: 10.1016/j.forsciint.2018.08.022

Marrone, A.; La Russa, D.; Barberio, L.; Murfuni, M. S.; Gaspari, M. and Pellegrino, D. (2023). Forensic Proteomics for the Discovery of New *postmortem* Interval Biomarkers: A Preliminary Study. International Journal of Molecular Science, 24(19), 14627. https://www.mdpi.com/1422-0067/24/19/14627

Mund, T.; Gewies, A.; Schoenfeld, N.; Bauer, M.K. and Grimm, S.S. (2003). Spike, a novel BH3-only protein, regulates apoptosis at the endoplasmic reticulum. The FASEB Journal, 17(6), 696–698. https://doi.org/10.1096/fj.02-0657fje

Nagata S. (1999). Fas ligand-induced apoptosis. Annual review of genetics; 33(1), 49-55. https://doi.org/10.1146/annurev.genet.33.1.29

Nolan, A.; Mead, R.; Maker, G. and Speers, S. (2020). A review of the biochemical products produced during mammalian decomposition with the purpose of determining the post1mortem interval. Australian Journal of Forensic Sciences, 52 (4), 477-488. https://doi.org/10.1080/00450618.2019.1589571

Noshy, P. (2021). Postmortem expression of apoptosis-related genes in the liver of mice and their use for estimation of the time of death. International Journal of Legal Medicine, 135, 539-545. https://link.springer.com/article/10.1007/s00414-020-02419-5

Ohkawa, H.; Ohishi, N. and Yagi, K. (1979). Assay for lipid peroxides in animal tissues by thiobarbituric acid reaction. Analytical biochemistry, 95(2), 351–358. https://doi.org/10.1016/0003-2697(79)90738-3

Ozturk, C.; Sener, M.T. and Sener, E. (2013). The investigation of damage in the muscle tissue with the oxidant/antioxidant balance and the extent of postmortem DNA damage in rats. Life Science Journal, 10(3), 1631–1637. https://hdl.handle.net/11436/4101

Paglia, D. E. and Valentine, W. N. (1967). Studies on the quantitative and qualitative characterization of erythrocyte glutathione peroxidase. The Journal of laboratory and clinical medicine, 70(1), 158–169. https://doi.org/10.5555/uri:pii:0022214367900765

Saber, T.M. and Ali, H.A. (2016). Expression of cell death genes estimates time since death in rats. Romanian Society of Legal Medicine, 24, 164-167. https://www.rjlm.ro/system/revista/39/164-167

Sakahira, H.; Enari, M. and Nagata S. (1998). Cleavage of CAD inhibitor in CAD activation and DNA degradation during apoptosis. Nature, 391(6662), 96-9. https://www.nature.com/articles/34214

Sakr, M.F.; El-Khalek, A.M.A.; Mohammad, N.S.; Abouhashem N.S.; Gaballah M. H. and Ragab H.M. (2023). Estimation of postmortem interval using histological and oxidative biomarkers in human bone marrow. Forensic Science, Medicine and Pathology. https://doi.org/10.1007/s12024-023-00753-9

Salerno, M.; Cocimano, G.; Roccuzzo, S.; Russo, I.; Piombino-Mascali, D.; Márquez-Grant, N. and Sessa, F. (2022). New trends in immunohistochemical methods to estimate the time since death: a review. Diagnostics, 12(9), 2114. https://doi.org/10.3390/diagnostics12092114

Sampaio-Silva, F.; Magalhaes, T.; Carvalho, F.; Dinis-Oliveira, R.J. and Silvestre, R. (2013). Profiling of RNA degradation for estimation of postmorterm interval. PLoS One, 8, 56-70. https://doi.org/10.1371/journal.pone.0056507

Sanderson T, Wild G, Cull AM, Marston J, Zardin G (2019). Immunohistochemical and Immunofluoresent techniques. In: Bancroft's Theory and Practice of Histological Techniques, 8th edn. Elsevier, Phialdelphia, pp 337–396.

Sener, M.T.; Suleyman, H.; Hacimuftuoglu,

A.; Polat, B.; Cetin, N.; Suleyman, B. and Akcay, F. (2012). Estimating the postmortem interval by the difference between oxidant/antioxidant parameters in liver tissue. Adv Clin Exp Med, 21(6), 727–733. https://europepmc.org/article/med/23457129

Shaaban A.A.; Farrag I.M. and Bayoumy E.S. (2017). Estimation of early postmortem interval by biochemical changes in brain and liver of rats using some oxidant and antioxidant parameters The Egyptian Journal of Forensic Sciences and Applied Toxicology. 17 (1). https://dx.doi.org/10.21608/ejfsat.2017.46108

Shaaban, A.; Farrag, I. and Bayoumy, E. (2017). Estimation of early postmortem interval by biochemical changes in brain and liver of rats using some oxidant and antioxidant parameters. Egyptian Journal of Forensic Science, Applied Toxicology, 17 (1), 147-162. https://dx.doi.org/10.21608/ejfsat.2017.46108

Sharma, R.K. and Agarwal, A. (2004). Role of reactive oxygen species in gynecologic diseases. Reproductive medicine and Biology, 4, 177-199.

Sneeboer, M. A. M.; Snijders, G. J. L. J.; Berdowski, W. M.; Andreu, A.; Mierlo, H. C. and Berlekom, A. B. V. (2019). Microglia in post-mortem brain tissue of patients with bipolar disorder are not immune activated. Journal of Translational Psychiatry, 9(1), 153 https://doi.org/10.1038/s41398-019-0490-x

Soliman, A. A. A. A.; Haggag, O. G.; Sharaf Eldin, A. A. E.; Abdullah, O. A. S. and Ali, N. E. M. (2024). Role of biomarkers in determination of Wound Age: Histopathological, Immunohistochemical and molecular Study. Zagazig Journal of Forensic Medicine and Toxicology, 22(1), 177-204. https://dx.doi.org/10.21608/zjfm.2023.247011.1170

Tamura, M.; Gu J; Tran, H. and Yamada, K.M. (1999). PTEN gene and integrin signaling in cancer. Journal of National Cancer Institute, 91(21), 1820-8. https://doi.org/10.1093/jnci/91.21.1820

Tomassini, L.; Lancia, M.; Scendoni, R.; Manta, A. M.; Fruttini, D.; Terribile, E. and Gambelunghe, C. (2024). Dating Skin Lesions of Forensic Interest by Immunohistochemistry and Immunofluorescence Techniques: A Scoping Literature Review. Diagnostics, 14(2), 168. https://doi.org/10.3390/diagnostics14020168

Yahia, D.; El-Amir, Y. O. and Sadek, A. A. I. (2018). Early postmortem biochemical and histopathological changes in the kidney, liver, and muscles of dogs. Comparative Clinical Pathology, 27, 1447-1455. https://link.springer.com/article/10.1007/s00580-018-2756-8

Yilmaz, M.; Isaoglu, U.; Cetin, N.; Turan, M.I.; Suleyman, B.; Gocer, F.; Ozgeris, F.B. and Suleyman, H. (2012). Effects of adrenalin on ovarian injury formed by ischemia reperfusion in rats. Lat Am J Pharm, 31(7), 1032–1037.

Youssef, G.; Waheed, R.; Ibrahim, S.; Khalifa, O. (2019). Evaluation the Time of Death by Different Markers in Liver and Brain of Rats. Indian Journal of Forensic Medicine & Toxicology, 13 (4), 458. https://doi.org/10.5958/0973-9130.2019.00330.X

Zadka, Ł.; Chrabaszcz, K.; Buzalewicz, I.; Wiercigroch, E.; Glatzel-Plucińska, N.; Szleszkowski, Ł.; Gomułkiewicz, A.; Piotrowska, A.; Kurnol, K. and Dzięgiel, P. (2021). Molecular profiling of the intestinal mucosa and immune cells of the colon by multi-parametric histological techniques. Scientific Reports, 11, 11309. https://www.nature.com/articles/s41598-021-90761-y

Zapico CS, Menendez ST, Nunez P. (2014). Cell death proteins as markers of early postmortem interval. Cellular and Molecular Life Science, 71(15), 2957-62. https://link.springer.com/article/10.1007/s00018-013-1531-x

Zapico, S.; Menéndez, S. and Núñez, P. (2014). Cell death proteins as markers of early postmortem interval. Cellular and Molecular Life Sciences, 71, 2957–2962. https://doi.org/10.1007/s00018-013-1531-x.

تقدير فترة ما بعد الوفاة باستخدام مؤشرات عديدة في كبد الجرذان البيضاء البالغة (تحديدا مسار اشاره PTEN/FasL)

رباب فوزي هنداوي[1] إيمان محمد فاروق [2] سامية مناوي[3] بسمة أحمد إبراهيم[4] دعاء السيد عبد الرزاق[5] نهلة محمد ابراهيم[5]
قسم الطب الشرعي والسموم الاكلينيكية كلية الطب البشري جامعة بنها مصر[1]
قسم التشريح كلية الطب البشري جامعة ام القرى المملكة العربية السعودية [2]
قسم التشريح وعلم الأجنة كلية الطب البشري جامعه بنها مصر[3]
قسم الكيمياء الحيوية الطبية والبيولوجيا الجزيئيه كلية الطب البشري جامعة الزقازيق مصر[4]
قسم الطب الشرعي والسموم كلية الطب البشري جامعة الزقازيق مصر[5]

المقدمة: يعد تقدير الفترة ما بعد الوفاة من أهم القضايا في مجال العلوم الطبية الشرعية. وتحدث بعد الوفاة تغييرات كيميائية حيوية مما يسبب الموت الخلوي. **الهدف:** تقييم التغيرات في عوامل الأكسدة ومضادات الأكسدة وكذلك تقييم التعبيرعن mRNA في مسار موت الخلية والتغيرات الكيميائية المناعية في كبد الجرذان بعد الوفاة. **الطريقة:** شملت هذه الدراسة خمسة وثلاثون من الجرذان البيضاء البالغة مقسمة إلى خمس مجموعات متساوية. تم استخراج كبد الجرذان لكل المجموعات على فترات (٠, ٣, ٦, ١٢, ٢٤) ساعة بعد الوفاة لقياس دلالات الإجهاد التأكسدي MDA وCatalase و GPx وقياس مستوى التعبير عن mRNA لكل من FASL\PTEN\Bax\Caspase3باستخدام PCR الكمي. وكذلك تحديد التغيرات الكيميائية المناعية في الأنسجة. **النتائج:** أشارت النتائج الى ارتفاع ملحوظ في عامل الأكسدة MDA وانخفاض في مستويات مضادات الأكسدة Catalase بعد مرور ٣ ساعات و GPx بعد مرور٦ ساعات بعد الوفاة. كما تدل النتائج على علاقة طردية ذات دلالة احصائية مع مستوى الجينات FasL\PTEN\Bax\Caspase-3في كبد الجرذان بينما توجد علاقة عكسية ذات دلالة احصائية في مستوىBcl2. **الخلاصة:** خلصت هذه الدراسة إلى أن عوامل الأكسدة ومضادات الأكسدة وعوامل التحلل الذاتي والمتضمنة في آلية إشارات موت الخلايا يمكن استخدامها في تحديد الفترة المبكرة بعد الوفاة. **التوصيات:** إجراء المزيد من البحوث مع الأخذ في الاعتبار العوامل الاخري ذات الصلة بعملية التحلل الذاتي بعد الوفاة. كما يوصى بأن تكون هذه العوامل موضوعا لمزيد من الدراسات على الحيوانات لمدة مختلفة وكذلك على البشر.